

Dear Dr/Prof. S.B. Saidman,

Here are the proofs of your article.

- You can submit your corrections **online** or by **fax**.
- For **online** submission please insert your corrections in the online correction form. Always indicate the line number to which the correction refers.
- For **fax** submission, please ensure that your corrections are clearly legible. Use a fine black pen and write the correction in the margin, not too close to the edge of the page.
- Please return your proof together with the **permission to publish** confirmation.
- Remember to note the journal title, article number, and your name when sending your response via e-mail, fax or regular mail.
- **Check** the metadata sheet to make sure that the header information, especially author names and the corresponding affiliations are correctly shown.
- **Check** the questions that may have arisen during copy editing and insert your answers/ corrections.
- **Check** that the text is complete and that all figures, tables and their legends are included. Also check the accuracy of special characters, equations, and electronic supplementary material if applicable. If necessary refer to the *Edited manuscript*.
- The publication of inaccurate data such as dosages and units can have serious consequences. Please take particular care that all such details are correct.
- Please **do not** make changes that involve only matters of style. We have generally introduced forms that follow the journal's style. Substantial changes in content, e.g., new results, corrected values, title and authorship are not allowed without the approval of the responsible editor. In such a case, please contact the Editorial Office and return his/her consent together with the proof.
- If we do not receive your corrections **within 48 hours**, we will send you a reminder.

Please note

Your article will be published **Online First** approximately one week after receipt of your corrected proofs. This is the **official first publication** citable with the DOI. **Further changes are, therefore, not possible.**

After online publication, subscribers (personal/institutional) to this journal will have access to the complete article via the DOI using the URL: [http://dx.doi.org/\[DOI\]](http://dx.doi.org/[DOI]).

If you would like to know when your article has been published online, take advantage of our free alert service. For registration and further information go to: www.springerlink.com.

Due to the electronic nature of the procedure, the manuscript and the original figures will only be returned to you on special request. When you return your corrections, please inform us, if you would like to have these documents returned.

The **printed version** will follow in a forthcoming issue.

**Fax to: +44 207 806 8278 or +44 870 762 8807 (UK)
or +91 44 4208 9499 (INDIA)**

To: Springer Correction Team

6&7, 5th Street, Radhakrishnan Salai, Chennai, Tamil Nadu, India – 600004

Re: Journal of Applied Electrochemistry DOI:10.1007/s10800-008-9489-3
Polarisation behaviour of Al–Zn–Ga alloy in chloride medium

Authors: D.O. Flamini · S.B. Saidman

Permission to publish

I have checked the proofs of my article and

- I have no corrections. The article is ready to be published without changes.
- I have a few corrections. I am enclosing the following pages:
- I have made many corrections. Enclosed is the complete article.

Date / signature _____

ELECTRONIC REPRINT ORDER FORM

After publication of your journal article, electronic (PDF) reprints may be purchased by arrangement with Springer and Aries Systems Corporation.

The PDF file you will receive will be protected with a copyright system called DocuRights®. Purchasing 50 reprints will enable you to redistribute the PDF file to up to 50 computers. You may distribute your allotted number of PDFs as you wish; for example, you may send it out via e-mail or post it to your website. You will be able to print five (5) copies of your article from each one of the PDF reprints.

Please type or print carefully. Fill out each item completely.

1. Your name: _____
 Your e-mail address: _____
 Your phone number: _____
 Your fax number: _____
2. Journal title (vol, iss, pp): _____
3. Article title: _____
4. Article author(s): _____
5. How many PDF reprints do you want? _____
6. Please refer to the pricing chart below to calculate the cost of your order.

Number of PDF reprints	Cost (in U.S. dollars)
50	\$200
100	\$275
150	\$325
200	\$350

NOTE: Prices shown apply only to orders submitted by individual article authors or editors. Commercial orders must be directed to the Publisher.

All orders must be prepaid. Payments must be made in one of the following forms:

- a check drawn on a U.S. bank
- an international money order
- Visa, MasterCard, or American Express (no other credit cards can be accepted)

PAYMENT (type or print carefully):

Amount of check enclosed: _____ (payable to Aries Systems Corporation)

VISA _____

MasterCard _____

American Express _____

Expiration date: _____ Signature: _____

Print and send this form with payment information to:

Aries Systems Corporation
 200 Sutton Street
 North Andover, Massachusetts 01845
 Attn.: Electronic Reprints
 — OR —
 Fax this to Aries at: 978-975-3811

Your PDF reprint file will be sent to the above e-mail address. If you have any questions about your order, or if you need technical support, please contact: support@docurights.com

For subscriptions and to see all of our other products and services, visit the Springer website at:

<http://www.springeronline.com>

Metadata of the article that will be visualized in OnlineFirst

ArticleTitle	Polarisation behaviour of Al–Zn–Ga alloy in chloride medium	
Article Sub-Title		
Article CopyRight - Year	Springer Science+Business Media B.V. 2008 (This will be the copyright line in the final PDF)	
Journal Name	Journal of Applied Electrochemistry	
Corresponding Author	Family Name	Saidman
	Particle	
	Given Name	S. B.
	Suffix	
	Division	Instituto de Ingeniería Electroquímica y Corrosión (INIEC), Departamento de Ingeniería Química
	Organization	Universidad Nacional del Sur
	Address	Av. Alem, 1253, 8000, Bahía Blanca, Argentina
	Email	ssaidman@criba.edu.ar
Author	Family Name	Flamini
	Particle	
	Given Name	D. O.
	Suffix	
	Division	Instituto de Ingeniería Electroquímica y Corrosión (INIEC), Departamento de Ingeniería Química
	Organization	Universidad Nacional del Sur
	Address	Av. Alem, 1253, 8000, Bahía Blanca, Argentina
	Email	
Schedule	Received	29 August 2007
	Revised	5 January 2008
	Accepted	11 January 2008
Abstract	The electrochemical response of Al–Zn–Ga alloy in chloride medium was studied. For this purpose, linear sweep voltammetry and open circuit potential (OCP) measurements were employed and surface characterisation was performed by scanning electron microscopy (SEM) and energy dispersive X-ray (EDX) analysis. The presence of Ga whether as alloyed element in the ternary alloy or deposited from the electrolyte solution onto pure Al or onto Al–Zn alloy causes a displacement of the onset of the process of dissolution towards more negative potential in a chloride solution. The anodic behaviour of the Al–Zn–Ga alloy can be interpreted in terms of an amalgam mechanism, where the homogeneous distribution of Ga in the alloy assures the formation of a superficial Ga–Al amalgam.	
Keywords (separated by '-')	Al–Zn–Ga alloy - Aluminium - Gallium - Activation mechanism - Amalgam	
Footnote Information		

Polarisation behaviour of Al–Zn–Ga alloy in chloride medium

D. O. Flamini · S. B. Saidman

Received: 29 August 2007 / Revised: 5 January 2008 / Accepted: 11 January 2008
© Springer Science+Business Media B.V. 2008

Abstract The electrochemical response of Al–Zn–Ga alloy in chloride medium was studied. For this purpose, linear sweep voltammetry and open circuit potential (OCP) measurements were employed and surface characterisation was performed by scanning electron microscopy (SEM) and energy dispersive X-ray (EDX) analysis. The presence of Ga whether as alloyed element in the ternary alloy or deposited from the electrolyte solution onto pure Al or onto Al–Zn alloy causes a displacement of the onset of the process of dissolution towards more negative potential in a chloride solution. The anodic behaviour of the Al–Zn–Ga alloy can be interpreted in terms of an amalgam mechanism, where the homogeneous distribution of Ga in the alloy assures the formation of a superficial Ga–Al amalgam.

Keywords Al–Zn–Ga alloy · Aluminium · Gallium · Activation mechanism · Amalgam

1 Introduction

Aluminium is unsuitable as a sacrificial anode in cathodic protection systems as well as anode material in batteries due to the spontaneous formation of a passivating oxide. The incorporation of alloying elements such as Hg, Zn, In and Ga is used to shift the potential towards sufficiently electronegative values. Some work has been conducted to study the effects imparted by Ga when alloyed with Al or when present as an ion in solution [1–4].

There is general agreement that Ga accelerates anodic dissolution of Al and several mechanisms have been proposed to account for this. It has been suggested that Ga allows chloride adsorption at more negative potentials [3, 4]. It has also been proposed that Ga particles at the metal/oxide interface cause local thinning of the passive oxide film [1]. In a previous paper an amalgam-activation mechanism was proposed which needs a minimum amount of quasi-liquid Ga in true metallic contact with Al [5]. Gallium surface diffusion undermines and detaches the Al oxide, increasing the active area. Al oxidation at the amalgam/solution interface gives an active potential. The presence of Zn electrodeposited from the solution or as an alloying component assures that the critical surface concentration of Ga needed to activate is reached.

Although several studies have been carried out on the corrosion of Al–Zn–In alloys [6–8], the electrochemical behaviour of the Al–Zn–Ga alloy has received little attention [9]. Continuing the work on the activation process of Al in the presence of Ga and Zn, the electrochemical behaviour of the Al–Zn–Ga alloy is reported here. Potentiodynamic and open circuit potential (OCP) measurements are employed and surface characterisation is performed by scanning electron microscopy (SEM) and energy dispersive X-ray analysis (EDX). Electrochemical impedance spectroscopy (EIS) was used to comparatively study the corrosion behaviour of pure Al and Al–Zn in chloride media in the presence of Ga^{3+} with that of the ternary alloy.

2 Experimental details

Disc electrodes made from pure Al, Al–3.9%Zn and Al–5.6%Zn–3.0%Ga alloys embedded in a Teflon holder were used as working electrodes. Alloys were obtained

A1 D. O. Flamini · S. B. Saidman (✉)
A2 Instituto de Ingeniería Electroquímica y Corrosión (INIEC),
A3 Departamento de Ingeniería Química, Universidad Nacional
A4 del Sur, Av. Alem, 1253, 8000 Bahía Blanca, Argentina
A5 e-mail: ssaidman@criba.edu.ar

65 using pure metals (99.99%, Aldrich Chemical Co.). The
 66 discs were polished with 1000 grit SiC emery paper followed
 67 by 1 μm and 0.3 μm grit alumina suspensions and then
 68 cleaned with triply distilled water. The auxiliary electrode
 69 was a large Pt sheet. Potentials were measured against a SCE
 70 reference electrode connected through a Luggin–Haber
 71 capillary tip and are thus given throughout this work.

72 Linear sweep voltammetry at 0.005 V s^{-1} , initiating at
 73 the more negative potential, were applied to electrodes either
 74 still or under rotation. Electrochemical experiments were
 75 carried out using a potentiostat–galvanostat (PAR Model
 76 273 A) and a potentiostat–galvanostat (Voltalab 40 Model
 77 PGZ 301). A dual stage ISI DS 130 SEM and an EDAX 9600
 78 quantitative energy dispersive X-ray analyser were used to
 79 examine the electrode surface characteristics. Ac impedance
 80 spectra were recorded when the open circuit potential was
 81 stabilised, using an excitation voltage of 10 mV. The frequ-
 82 ency range studied was between 10 kHz and 10 mHz.

83 Chloride solutions (0.5 M NaCl) containing 0.01 M
 84 Ga^{3+} were prepared and the pH was adjusted to 2.5 with
 85 HCl. All chemicals were reagent grade and solutions were
 86 freshly made in triply-distilled water. Measurements were
 87 performed in a purified nitrogen gas saturated atmosphere.

88 3 Results and discussion

89 The voltammogram of Al–Zn–Ga in 0.5 M NaCl, pH 2.5
 90 solution between -2 V and -1.2 V at 0.005 V s^{-1} is pre-
 91 sented in Fig. 1, curve a. A current peak can be observed at
 92 the more negative potentials. This peak may be due to the
 93 summation of hydrogen evolution and Al dissolution which
 94 occur at the same electrode potentials [10]. At more positive
 95 potentials, a passive region is observed followed by a sharp
 96 current increase. The anodic current begins at -1.36 V ,
 97 consistent with the OCP (Fig. 2a). The active behaviour
 98 initiates practically at the same potential in the pH range

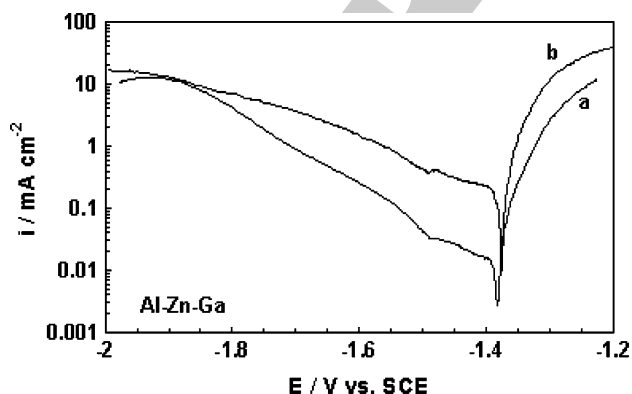


Fig. 1 Voltammogram of Al–Zn–Ga alloy at 0.005 V s^{-1} in a 0.5 M NaCl, pH 2.5 solution: (a) without Ga^{3+} and (b) with 0.01 M Ga^{3+}

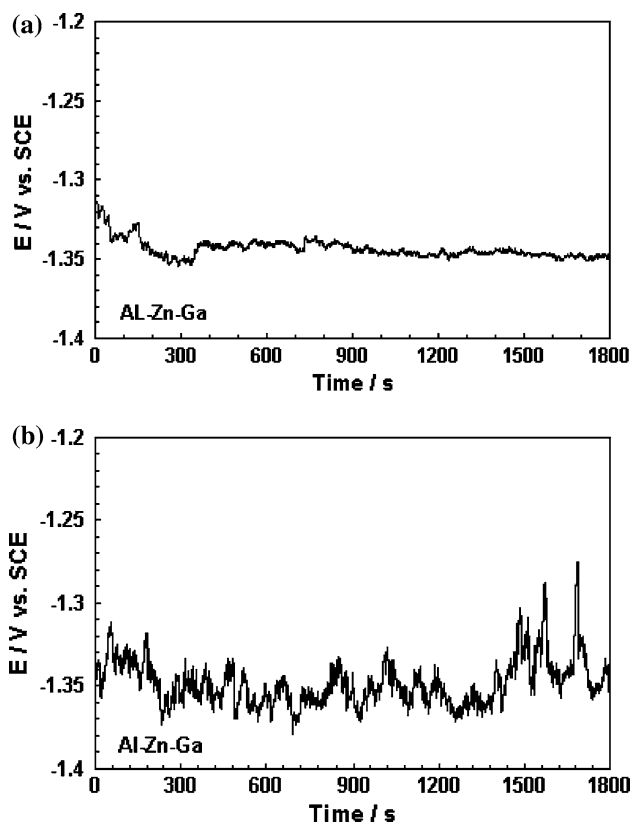


Fig. 2 Open circuit potential vs. time plot of Al–Zn–Ga alloy in a 0.5 M NaCl, pH 2.5 solution at (a) $25\text{ }^{\circ}\text{C}$ and (b) $60\text{ }^{\circ}\text{C}$

2.5 \leq pH \leq 6. The response corresponding to the Al–Zn–Ga alloy in the presence of Ga^{3+} is also included (Fig. 1, curve b). An increased cathodic current is measured which is associated with the deposition of Ga. Although the anodic current initiates at practically the same potential as in the absence of the activator, the anodic dissolution is significantly depolarised when Ga^{3+} is added to the solution.

The influence of temperature was also analysed. It was found that the OCP vs. time plot (Fig. 2b), as well as the voltammogram (Fig. 3) at $60\text{ }^{\circ}\text{C}$ in a 0.5 M NaCl, pH 2.5

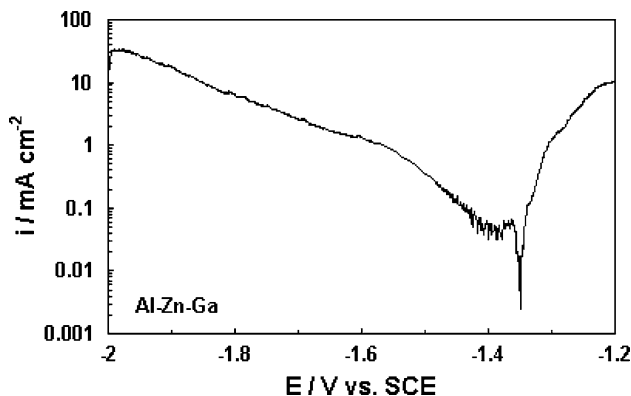


Fig. 3 Voltammogram of Al–Zn–Ga alloy at 0.005 V s^{-1} in a 0.5 M NaCl, pH 2.5 solution at $60\text{ }^{\circ}\text{C}$

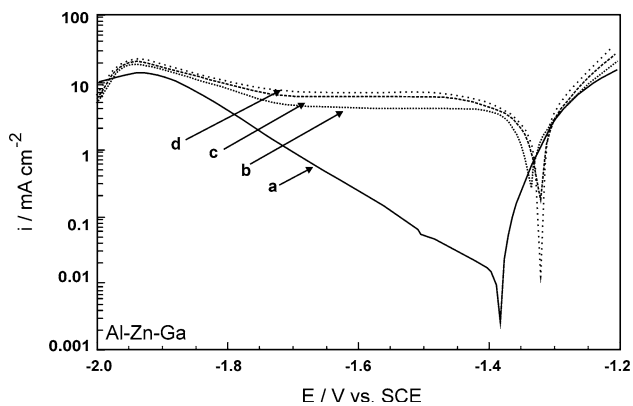


Fig. 4 Voltammogram of Al-Zn-Ga alloy at 0.005 V s^{-1} in a 0.5 M NaCl , $\text{pH } 2.5$ solution at different rotation rates: (a) 0 rpm , (b) 500 rpm , (c) 1000 rpm and (d) 1500 rpm

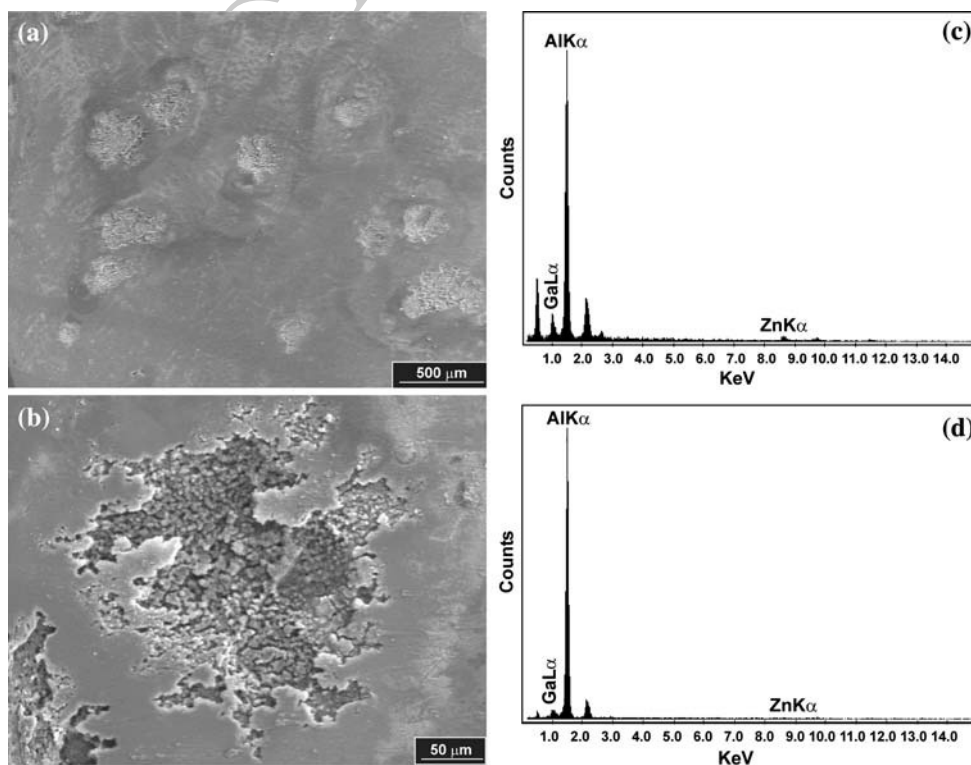
109 solution, are almost identical with those obtained at $25 \text{ }^\circ\text{C}$.
 110 In the case of Al-Zn-In it is postulated that the exothermic
 111 hydrolysis reaction of the Al^{3+} ions provides a sufficiently
 112 high temperature to promote the presence of quasi-liquid In
 113 [8]. This fact and the low melting point of Ga explain the
 114 independence of the electrochemical behaviour of the Al-
 115 Zn-Ga alloy with solution temperature.
 116 If the electrode is rotated during the potential scan
 117 the shape of the polarisation curve is similar to that
 118 obtained without rotation but higher currents, both anodic
 119 and cathodic, are measured as the rotation rate increases

(Fig. 4). Moreover, the corrosion potential is independent
 of the rotation rate.

Figure 5 shows the SEM/EDX examination of the ternary alloy surface polarised from -2 V to -1 V at a scan rate of 0.005 V s^{-1} . The attacked areas are uniformly distributed (Fig. 5a). A close view of these areas shows irregular, non-crystallographic, probably tunnel-like pits (Fig. 5b). This morphology is similar to that found for the Al-Zn alloy [11], although for the ternary alloy investigated here pits are not deep. Moreover, the cavities are covered with a cracked film. In the case of the Al-Zn-In alloy the attack initiates and propagates in those zones enriched in In and Zn during the solidification process, i.e., grain boundaries and interdendritic zones [8]. The low solubility of In in the Al matrix according to the binary alloy phase diagrams (0.19 wt\% In) explains this segregation [12]. Conversely, the higher solubility of Ga in Al (2 wt\%) [12] explains the homogeneous distribution of the attacked areas. The more uniform pitting distribution ensures higher current efficiency, which constitutes a requirement for a sacrificial anode. EDX analysis performed inside the damaged areas (Fig. 5c) showed increasing amounts of Ga (7.72 wt\%) and Zn (18.83 wt\%) compared to the rest of the electrode surface (Fig. 5d). This accumulation indicates that preferential Al dissolution takes place in the attacked area.

The average corrosion potential of the ternary alloy under study in acid chloride solution (-1.34 V) indicates an active

Fig. 5 (a) SEM micrograph showing the attacked areas uniformly distributed onto electrode surface of Al-Zn-Ga alloy, (b) magnified SEM image of the attacked area, (c) EDX spectrum inside of the attacked area and (d) EDX spectrum outside of the attacked area



148 state. A nominal composition of 2.6% Ga was used because
 149 this percentage assures an activated Al–Ga alloy [13]. The
 150 onset of anodic currents in the i/E curve of the ternary alloy
 151 presented in Fig. 1 practically matches that of the Al–Zn
 152 alloy in the presence of Ga^{3+} . Figure 6 shows the voltam-
 153 mogram in the anodic direction at 0.005 V s^{-1} for an Al–Zn
 154 alloy after different polarisation times at -2 V . The
 155 voltammetric curves show an anodic peak which is attrib-
 156 utable to an activation process by amalgam depassivation
 157 control [5], where Al incorporation and diffusion within
 158 the amalgam is followed by its oxidation at the amalgam/
 159 solution interface. The agreement between the onsets of the
 160 anodic currents for both systems suggests that in the case of
 161 the ternary alloy the Ga–Al amalgam is also responsible for
 162 activation. The presence of Ga as an alloying component
 163 promotes and maintains the active state. At higher anodic
 164 potentials, around -1.1 V , the presence of Ga facilitates
 165 chloride adsorption and then the pitting process ensues.

166 For a better assessment of the activation process addi-
 167 tional information was obtained by using EIS. The Nyquist
 168 diagram for the ternary alloy without electrode rotation
 169 shows a slightly depressed semicircle followed by a tail in the
 170 low frequency range (Fig. 7, curve a). In principle the
 171 impedance spectra in the high frequency range can be
 172 interpreted by a simple Randles circuit comprising a parallel
 173 combination of a resistor representing the charge-transfer
 174 resistance (R_{ct}) and a capacitor representing the electrode
 175 capacitance (C), in series with a resistor representing the
 176 ohmic drop in the electrolyte solution. (R_s). The R_{ct} is
 177 directly associated with the rate of the electrochemical cor-
 178 rosion reaction [14]. Because of the low value of R_s , R_{ct} can
 179 be determined by extrapolation of the semicircle up to the
 180 real axis. The semicircle depression in the Nyquist plot is
 181 attributable to surface heterogeneity and/or roughness.

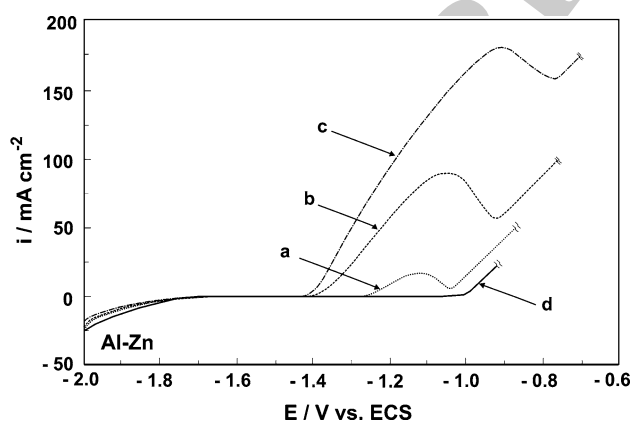


Fig. 6 Voltammogram of Al–Zn alloy at 0.005 V s^{-1} in a 0.5 M NaCl , $\text{pH } 2.5$ solution with 0.01 M Ga^{3+} at different cathodic polarisation times at -2.0 V : (a) 60 s , (b) 600 s and (c) 1200 s . The voltammogram of Al–Zn alloy in a 0.5 M NaCl , $\text{pH } 2.5$ solution without Ga^{3+} after cathodic polarisation at -2.0 V during 10 min is also included (curve d)

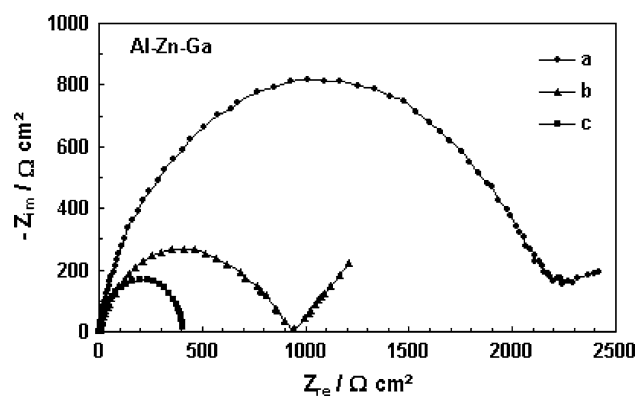


Fig. 7 Nyquist plots for Al–Zn–Ga alloy at open circuit potential condition in a 0.5 M NaCl , $\text{pH } 2.5$ solution: (a) without Ga^{3+} , (b) with 0.01 M Ga^{3+} and (c) without Ga^{3+} under electrode rotation (500 rpm)

182 According to Fig. 7, curve a, R_{ct} is $2.21 \text{ k}\Omega \text{ cm}^2$ and is
 183 smaller in the presence of Ga^{3+} ($0.9 \text{ k}\Omega \text{ cm}^2$) (Fig. 7, curve b)
 184 demonstrating that Ga^{3+} causes enhanced corrosion. When
 185 Ga^{3+} is dissolved in solution, greater amounts of the metal
 186 are deposited facilitating amalgam formation.

187 Under rotation the impedance of the Al–Zn–Ga alloy in
 188 chloride solution reduces to a semicircle with diameter
 189 equal to $0.4 \text{ k}\Omega \text{ cm}^2$ (Fig. 7, curve c) indicating a higher
 190 corrosion rate compared with that obtained under stagnant
 191 conditions. This result agrees with that obtained under
 192 potentiodynamic polarisation.

193 To gain a better understanding of the role of Ga and Zn
 194 on the corrosion behaviour of Al, impedance data were
 195 obtained for Al and Al–Zn electrodes in chloride solution
 196 with and without addition of the activator. The effect of
 197 varying the cathodisation time at -2.0 V on the polarisa-
 198 tion behaviour of Al in chloride solution containing Ga^{3+}
 199 was first analysed (Fig. 8). The pitting process initiates at

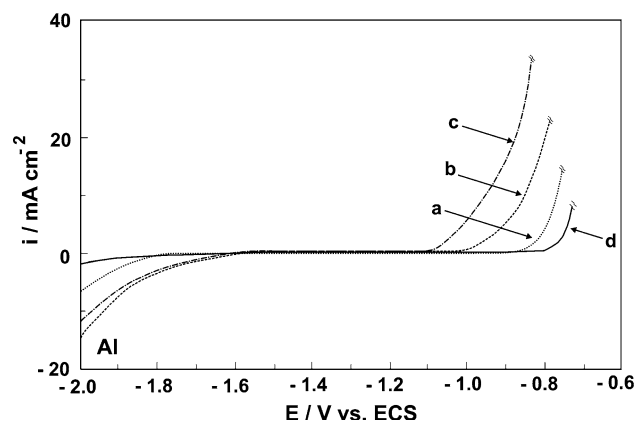


Fig. 8 Voltammogram of pure Al at 0.005 V s^{-1} in a 0.5 M NaCl , $\text{pH } 2.5$ solution with 0.01 M Ga^{3+} at different cathodic polarisation times at -2.0 V : (a) 60 s , (b) 600 s and (c) 1200 s . The voltammogram of pure Al in a 0.5 M NaCl , $\text{pH } 2.5$ solution without Ga^{3+} after cathodic polarisation at -2.0 V during 10 min is also included (curve d)

200 more negative potentials as the cathodisation time increases
 201 because higher amounts of Ga are deposited. A
 202 decrease in the semicircle diameter is observed when the
 203 Al electrode is held at -2.0 V (Fig. 9, curves a and b). This
 204 is explained by the oxide hydration/elimination by local
 205 alkalisation produced during hydrogen evolution on the
 206 Al surface. On the other hand, there are clear differences
 207 between the Nyquist plot obtained for bare Al and for the
 208 Al electrode with deposited Ga after cathodisation (Fig. 9,
 209 curves b and c). R_{ct} is reduced by almost an order of
 210 magnitude in the presence of deposited Ga, which is consistent
 211 with enhanced Al dissolution sustained by chloride
 212 adsorption produced by the presence of Ga at more negative
 213 potentials [3, 4, 15].

214 Figure 10 illustrates the EIS data of Al–Zn alloy with
 215 and without the activator. The overall impedance is
 216 significantly smaller for the alloy compared with that
 217 obtained for pure Al in agreement with enhanced Al
 218 dissolution in the presence of Zn [11, 16]. The Nyquist plot
 219 for the Al–Zn alloy in chloride solution shows two
 220 capacitive loops. The R_{ct} increases when Ga is deposited

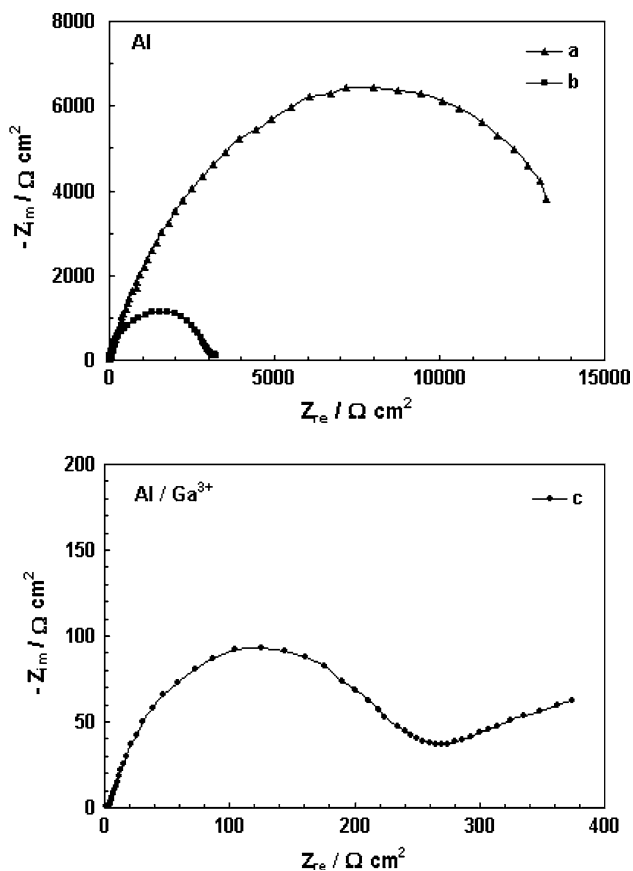


Fig. 9 Nyquist plots for pure Al at open circuit potential condition in a 0.5 M NaCl, pH 2.5 solution: (a) without previous cathodisation, (b) after cathodic polarisation at -2.0 V during 10 min and (c) after cathodic polarisation at -2.0 V during 10 min in the presence of 0.01 M Ga^{3+}

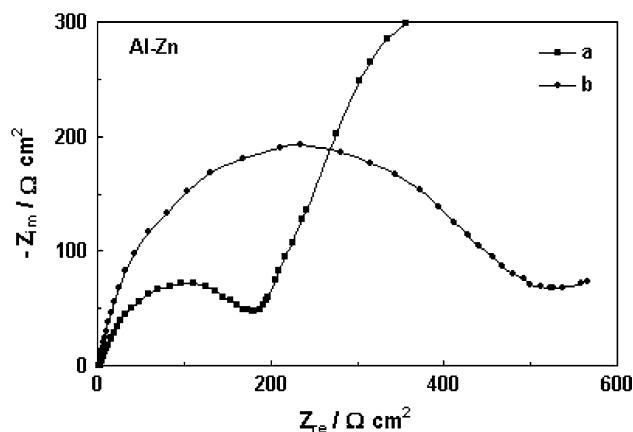


Fig. 10 Nyquist plots for Al–Zn alloy at open circuit potential condition in a 0.5 M NaCl, pH 2.5 solution after cathodic polarisation at -2.0 V during 10 min: (a) without Ga^{3+} and (b) with 0.01 M Ga^{3+}

221 onto the binary alloy. The reason for this change can be
 222 explained considering that different mechanisms are operative
 223 and consequently, different corrosion rates are expected.
 224 As already mentioned, the oxidation mechanism of the bare
 225 alloy is a chloride pitting process while it is possible to
 226 activate Al–Zn alloy via Ga–Al amalgam formation that
 227 occurs at more negative potentials. On the other hand,
 228 it is reasonable to suppose that the true electrochemically
 229 active areas are different for both processes.

230 The appearance of the second capacitive loop at the low
 231 frequency values in the plot corresponding to the binary
 232 Al–Zn alloy may be related to the precipitation of $\text{Zn}(\text{OH})_2$
 233 on the electrode surface [17]. It is reasonable to assume the
 234 same for the Al–Zn–Ga alloy, considering the similarities
 235 between the diagrams from the binary and ternary alloys.
 236 The suppression of the second capacitive loop under
 237 electrode rotation for the ternary alloy (Fig. 7, curve c),
 238 supports this because, in this case, corrosion product
 239 accumulation is hindered. Likewise, polarisation resistance
 240 is reduced under rotation, and this decrease is attributable
 241 to the difficulty in forming protective corrosion products.

4 Conclusions

242
 243 Activation of the Al–Zn–Ga alloy investigated takes place
 244 at potentials where adsorption of chloride is not feasible.
 245 This process can be interpreted in terms of an amalgam
 246 mechanism. The alloyed Ga homogeneously distributed
 247 assures the formation of the Ga–Al amalgam. The attacked
 248 areas are uniformly distributed and are not deep. The
 249 material is able to provide higher currents when the amount
 250 of Ga deposited at the interface is increased by electro-
 251 deposition from the solution. Accumulation of corrosion
 252 products is reduced under rotation, giving higher corrosion
 253 rates.

254 EIS measurements allowed comparison of the activating
 255 effect exerted by Ga and Zn on the electrochemical
 256 behaviour of Al and confirmation of the mechanisms out-
 257 lined previously for activation. The corrosion currents for
 258 the ternary alloy as well as for the Al–Zn alloy with Ga
 259 deposition are smaller than that of the bare Al–Zn alloy.
 260 This may be explained considering that the oxidation
 261 reaction changes from an amalgam-controlled dissolution
 262 to a pitting process.

263 **Acknowledgments** Financial support by the Secretaría de Ciencia y
 264 Técnica-UNS (PGI 24/M093/04) and the Consejo Nacional de
 265 Investigaciones Científicas y Técnicas (CONICET- PIP02143/00) is
 266 gratefully acknowledged.

267 References

268 1. Tuck CDS, Hunter JA, Scamans GM (1987) *J Electrochem Soc*
 269 134:2970

2. Mance A, Cerović D, Mihajlović A (1985) *J Appl Electrochem* 270
 15:415 271
 3. Breslin CB, Carroll WM (1992) *Corros Sci* 33:1735 272
 4. El Shayeb HA, Abd El Wahab FM, Zein El Abedin S (2001) 273
Corros Sci 43:643 274
 5. Flamini DO, Saidman SB, Bessone JB (2007) *Thin Sol Films* 275
 515:7880 276
 6. Breslin CB, Friery LP, Carroll WM (1994) *Corros Sci* 36:85 277
 7. Venugopal A, Angal Rd, Raja VS (1996) *Corrosion* 52:138 278
 8. Muñoz AG, Saidman SB, Bessone JB (2002) *Corros Sci* 44:2171 279
 9. Aragon E, Cazenave-Vergez L, Lanza E, Giroud A, Sebaoun A 280
 (1997) *Brit Corros J* 32:263 281
 10. Tomcsányi L, Nagy Zs, Somlai J, Borszéki J (1993) *Electrochim* 282
Acta 38:2541 283
 11. Muller IL, Galvele JR (1977) *Corros Sci* 17:995 284
 12. Baker H (1992) *ASM handbook*, vol 3. Alloy phase diagrams, 285
 Ohio 286
 13. Breslin CB, Carroll WM (1992) *Corros Sci* 33:1735 287
 14. Rosalbino F, Angelini E, Macciò D, Saccone A, Delfino S (2007) 288
Electrochim Acta 52:7107 289
 15. Flamini DO, Saidman SB, Bessone JB (2006) *Corros Sci* 48:1413 290
 16. Sato F, Newman RC (1999) *Corrosion* 55:3 291
 17. Shibli SMA, George S (2007) *Appl Surf Sci* 253:7510 292
 293